CHAPTER 5

SHORTWAVE RADIATION GEOMETRY AND GLACIER DISTRIBUTION IN THE CORDILLERA REAL, BOLIVIA

Abstract

Solar radiation is a primary energy source for ablation of the glaciers in the Cordillera Real of Bolivia (Francou *et al.*, 1995). However to date, no studies have quantitatively examined the spatial variation of shortwave radiation in the region and its relationship to glacier locations. The direct and diffuse shortwave radiation fields were computed using a clear-sky radiation model for a small area in the Huayna Potosí region (16 º17´ S, 68 º 12´ W) of the Cordillera Real, Bolivia. Hourly simulations of the shortwave components for the 21st day of each month show that glacierized areas receive significantly less shortwave radiation than non-glacierized areas at equivalent elevations during most months of the year. Annual average differences in total shortwave radiation incident upon glacierized and non-glacierized areas range between 2-4 MJ m^{-2} day^{-1}.

Introduction

Solar radiation provides a large percentage of the energy available for ablation occurring on the high elevation glaciers of the subtropical central Andes. Increased incident shortwave radiation due to decreased cloud cover during ENSO events contributes to the marked glacier retreat occurring in the region (Francou *et al.*, 1995). The strong influence of radiation on glacial

mass balance suggests that spatial variations in the net radiation field should influence where glaciers are located within the region and potentially glacier response to climatic forcings. However, the effect of orientation (aspect) on glacier Equilibrium Line Altitudes or ELAs in Bolivia has previously been examined only qualitatively (e.g. Jordan, 1985). Glaciers with north-easterly aspects have been found to have the highest ELAs.. This configuration was attributed to two effects: (1) at these low southern hemisphere latitudes, slopes with northern aspects receive more insolation than slopes with southern aspects, and (2) an afternoon buildup of clouds causes shading of slopes with a westerly aspects during the afternoon hours (Jordan, 1985; Hastenrath, 1991).

This study presents a quantitative analysis of the spatial distribution of shortwave radiation testing the hypothesis that glacierized areas receive less solar insolation than non-glacierized areas. A digital elevation model (DEM) was used to compute the direct and diffuse shortwave radiance incident on sloping surfaces under clear-sky conditions. Hourly simulations for the 21st day of each month were used to calculate seasonal and annual averages of incident shortwave radiation.

A small (15 km x 17.5 km) region of the Cordillera Real was selected for this preliminary study (**Figure 5.1A**). The site, centered at (16 º17´ S, 68 º 12´ W), contains Cerro Huayna Potosí (6088 m), one of the higher massifs within the range, as well as numerous smaller peaks. Eighty-nine glaciers and perennial snow patches have been recognized within the study area.

Figure 5.1: **(A)** Landsat Thematic Mapper image (Band 4) of the study area. The numerous small glaciers in the area appear white in the image. Areas considered in the study are enclosed in black outlines and were taken from Jordan's (1991) glacial survey. **(B)** Greyscale image of average annual total (direct + diffuse) radiation received on each 100 x 100 meter pixel in MJ m^{-2} day^{-1}.

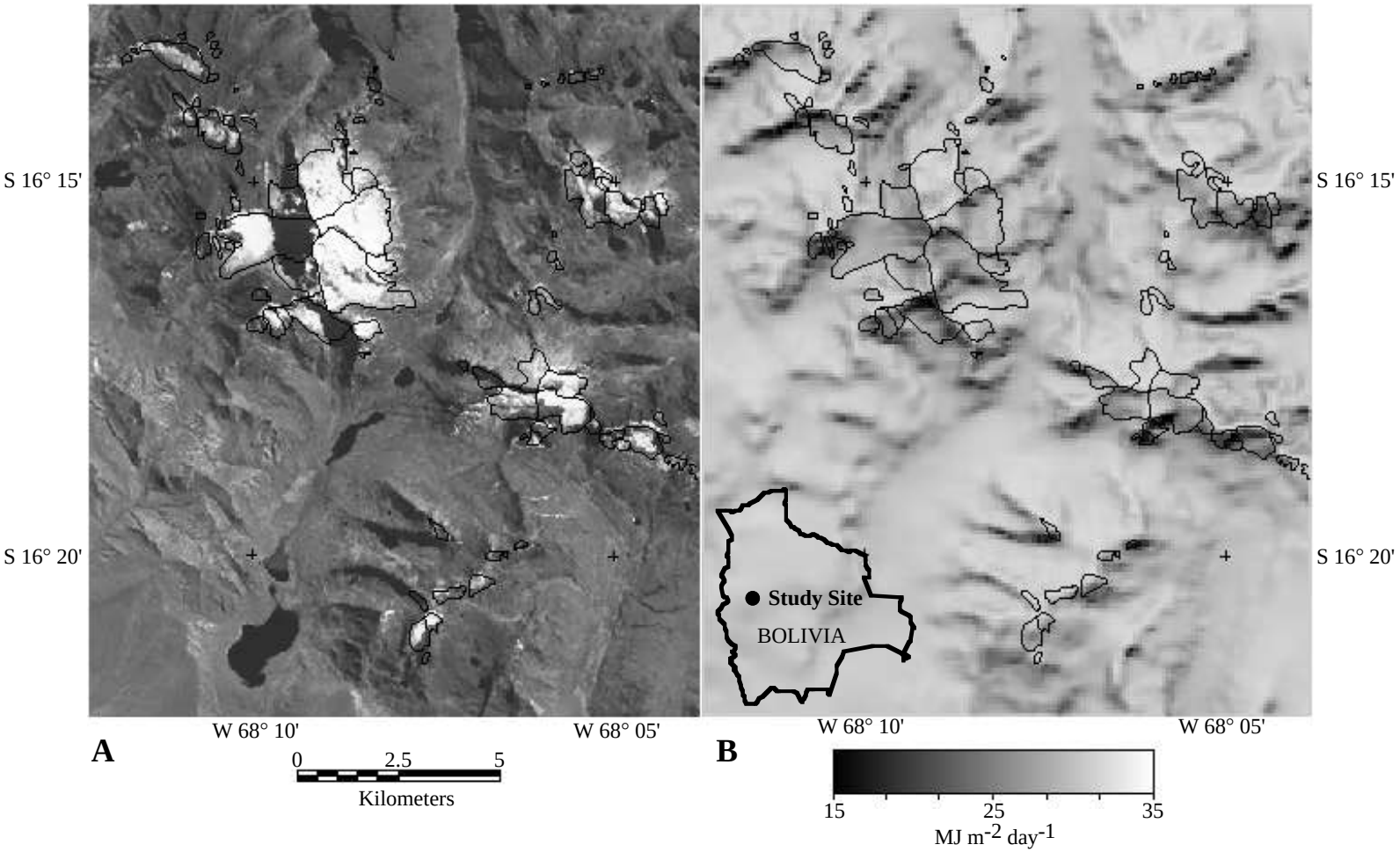
S 16° 15'
S 16° 20'
W 68° 10'
W 68° 05'
A
0
2.5
5
Kilometers
Study Site
BOLIVIA
B
15
25
35
MJ m-2 day-1

Glacierized areas were distinguished through digitization of 1:20,000 glacier maps produced by Jordan (1991).

Shortwave Terrain Modeling and Methodology

Mountainous terrain creates significant spatial variability in the incident shortwave radiation field. The total shortwave radiation incident upon a sloping surface is the sum of three components: direct, diffuse, and terrain reflectance. Direct radiation is a function of the elevation, slope, and aspect of each terrain facet, and whether the sun is obstructed from an individual terrain facet by surrounding topography. Diffuse radiation depends on the amount of the overlying sky visible to an individual slope facet. Terrain reflectance is neglected because of its relatively small magnitude and computational limitations in its calculation.

Topographically induced variations in shortwave radiation can be quantitatively modeled (e.g. Williams *et al.*, 1972) using digital elevation models (DEMs). The DEM for the study area was created from contours digitized from the 1:50,000 topographic maps produced by the Instituto Geografia Militar (IGM) in La Paz, Bolivia. The DEM, with 100 m resolution, was produced using a gridding algorithm developed by Hutchinson (1989) as implemented in the ARC/INFO® Geographic Information System. The slope and aspect of each cell were calculated from the DEM by a planar least-squares fit to the 9 adjacent elevation values within a 3x3 moving window.

Under clear-sky conditions the direct shortwave radiation (S_0) received on each terrain facet can be calculated as:

$$S_0 = I \eta \Phi T_r T_w \quad (1)$$

(Munro and Young, 1982) where I is the solar constant (1353 W m^{-2}), η is a binary shade factor (0 if the pixel is shadowed, 1 if not), Φ is the local illumination factor which corrects for topographic orientation, and T_r and T_w are atmospheric transmissivities accounting for Rayleigh scattering and water vapor absorption, respectively. The local illumination factor is calculated by:

$$\Phi = \cos(Z) \cos(\beta) + \sin(Z) \sin(\beta) \cos(\gamma_s - \gamma) \quad (2)$$

where Z is the solar zenith angle, β is the local topographic slope, γ is the local topographic aspect, and γ_s is the solar azimuth. The binary shade factor (η) utilizes the Dozier and Frew (1990) algorithm for rapid determination of local horizons.

The diffuse radiation (D_0) is calculated as:

$$D_0 = I \cos(Z) T_d V \quad (3)$$

The sky-view factor (V) is the fraction of the hemispheric sky dome visible from the given pixel (Dozier and Frew, 1990). It is calculated from the

DEM by calculating the horizon angle from each point on the topography in 8 directions (45° increments) and averaging.

The atmospheric transmissivities (T_r and T_w) are functions of atmospheric path length and hence decrease with increasing zenith angle and decreasing elevation. Expressions for T_r and T_w are taken from Coulson (1975) and Gruell and Oelermans (1986). T_d is the diffuse atmospheric transmissivity given by (Munro and Young, 1982) as:

$$T_d = \{0.5\ (1 - T_r)\} + \{0.8\ (1.0 - T_z)\ (T_r * T_w)\} \quad (4)$$

where T_z represents atmospheric dust transmissivity, fixed in this study at 0.95. The values of 0.5 and 0.8 represent forward scattering ratios for Rayleigh and Mie scattering, respectively (Munro and Young, 1982).

Results and Conclusions

Shortwave radiation geometry is found to be an important factor controlling the location of glaciers in the eastern Andes of Bolivia. Under clear-sky conditions, glaciers in the Huayna Potosí region are found preferentially in topographic positions receiving less incident solar radiation than non-glacierized areas. On an annual basis, mean differences in total (direct + diffuse) radiation received on glacierized and non-glacierized areas at the same elevation range between 2-4 MJ m^{-2} day^{-1}. These differences represent between 5 and 25 percent of the total radiation incident on glacierized slopes.

Despite the low latitude of the study site, the magnitude and the spatial patterns of incident shortwave radiation vary considerably from month to month. Incident net radiation averaged by elevation (**Figure 5.2A**) varies from 12 MJ m^{-2} day^{-1} during the austral winter months to over 35 MJ m-2 day-1 during austral summer months. Monthly mean differences in incident shortwave radiation between glacierized and non-glacierized areas also vary considerably throughout the year (**Figure 5.2B**). Maximum differences, up to 9 MJ m^{-2} day^{-1}, occur during the austral winter when absolute incident shortwave radiation is also low. Minimum differences are found during austral summer, when incident shortwave radiation is high in all landscape positions. From March to September, glacierized areas receive 10 to 50 percent less shortwave radiation than non-glacierized areas at equivalent elevation.

The occurrence of only negligible differences between incident solar radiation received on glacierized and non-glacierized slopes during the height of austral summer would seem to weaken the contention that spatial variations in the net shortwave field control glacier distribution. However, during austral summer little overall variation occurs in the shortwave field so it is not surprising that model results show only negligible differences in shortwave radiation received on glacierized and non-glacierized slopes. Increased cloudiness during this period also makes the clear-sky model less

Figure 5.2: **(A)** Average shortwave (direct + diffuse) insolation received on glacierized areas as a function of elevation for each month of the year. Each cell in the graph represents the mean monthly shortwave radiation for a 90 meter vertical interval. The contours indicate values of the incident radiation in MJ m^{-2} day^{-1}. **(B)** Mean monthly differences in total shortwave radiation between glacierized and non-glacierized areas as a function of elevation. Each cell represents the shortwave radiation difference for each month for the same 90 meter vertical interval shown in **(A)**. Differences are negative where glacierized areas receive less incident radiation. Contours indicate values of the incident radiation in MJ m^{-2} day^{-1}.

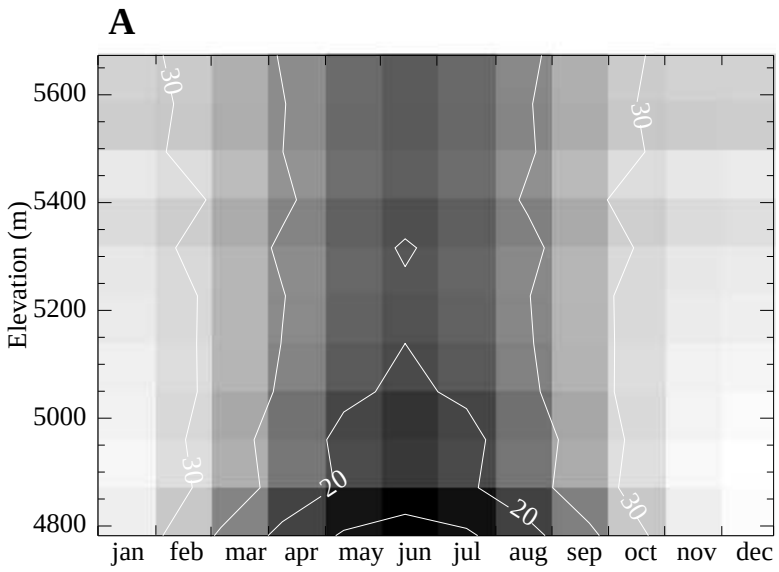
A
Elevation (m)
5600
5400
5200
5000
4800
jan
feb
mar
apr
may
jun
jul
aug
sep
oct
nov
dec
30
30
30
20
20
30

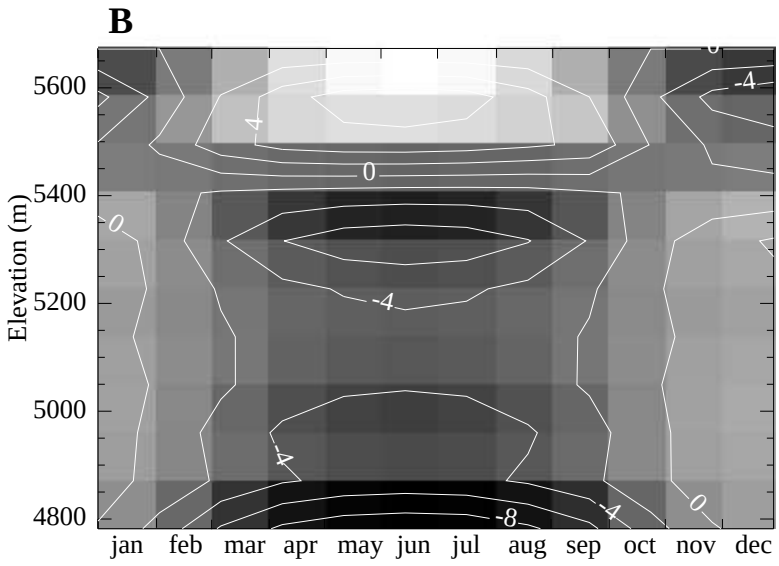
B
Elevation (m)
5600
5400
5200
5000
4800
jan
feb
mar
apr
may
jun
jul
aug
sep
oct
nov
dec
-4
4
0
0
-4
-4
-4
0
-8

representative of actual conditions than during the rest of the year. Most importantly, the early and late periods of the wet season (October-December and March-May) are the critical time periods for determining the annual mass balance of region's glaciers, especially during ENSO years (Francou *et al.*, 1995). Significant differences in incident shortwave radiation exist between glacierized and non-glacierized regions during most of these months, especially during March-May (**Figure 5.2B**).

In addition to differences in the direct component, significant differences in incident diffuse radiation occur between glacierized and non-glacierized areas. Assuming that diffuse radiation geometry is an adequate proxy for overcast skies, then under these conditions glacierized areas also receive less solar radiation than non-glacierized areas. This arises because glaciers tend to be located in topographic locations that 'see' a smaller portion of the overlying hemisphere.

The dominant southerly aspect of the majority of region's glaciers is the major reason glacierized areas receive less solar radiation than adjacent non-glacierized areas. On average, south facing slopes receive less annual shortwave radiation than northern slopes. Southerly slopes also exhibit higher variability in the magnitude of incident shortwave radiation for a given aspect. This is due to greater slope dependence of the direct component for locations facing away from the sun.

Considerable variation exists in the amount of average annual shortwave radiation incident upon individual glaciers. Differences in the average incident radiation received on the studied glaciers can be as large as 14 MJ m-2 day-1. Such differences could conceivably lead to varying glacier response to a climatic forcing. While this clear-sky modeling indicates radiation geometry influences the position of glaciers and creates large differences in the incident shortwave energy received on individual glaciers, inclusion of cloud cover in the model remains paramount in fully understanding the relationship between incident shortwave radiation and glaciers in the region.

Acknowledgments

This work is supported by NASA Mission to Planet Earth/Earth Observing System grant NAGW-2638. The first author is also supported by a DOE Graduate Fellowship for Global Change. The authors wish to thank Pierre Ribstein and Bernard Francou of ORSTOM/La Paz and Sophie Moreau of ABTEMA for their kind support. Thanks also to Christopher Duncan, Cornell University, for his indispensable software libraries. INSTOC contribution 224.

Bibliography

Coulson, K.L. (1975). *Solar and Terrestrial Radiation*. New York, Academic Press, 1975, 322 pp.

Dozier, J. and Frew, J. (1990). Rapid calculation of terrain parameters for radiation modeling from digital elevation data. *IEEE Transactions on Geoscience and Remote Sensing*, **28**(5), 963-969.

Francou, B., Ribstein, P., Saravia, R., and Tiriau, E. (1995). Monthly balance and water discharge of an inter-tropical glacier: Zongo, Glacier, Cordillera Real, Bolivia 16 ºS. *Journal of Glaciology*. **41**(137), 61-67.

Gruell, W. and Oerlemans, J. (1986). Sensitivity studies with a mass balance model including temperature profile calculations inside the glacier. *Zeitschrift für Gletscherkunde und Glazialgeologie,* **22**(2), 101-124.

Hastenrath, S. (1991). *Climate Dynamics of the Tropics*. Dordrecht, Kluwer Academic Publishers, 488 pp.

Hutchinson, M.F. (1989). A new procedure for gridding elevation and stream line data with automatic removal of spurious pits. *Journal of Hydrology*, **106**, 211-232.

Jordan, E. (1991). *Die Gletschcer der Bolivianischen Andean*. Stutgart, Franz Steiner Verlag, 365 pp.

Jordan, E. (1985). Recent glacier distribution and present climate in the central Andes of South America. *Zeitschrift für Gletscherkunde und Glazialgeologie*, **21**, 213-224.

Munro, G.J. and Young, D.S. (1982). An operational net shortwave radiation model for glacier basins. *Water Resources Research*, **18**(2), 220-230.

Williams, L.D., Barry, R.G., and Andrews, J.T., (1972). Application of computed global radiation for areas of high relief, *Journal of Applied Meteorology*, **11**, 526-533.